NASA Technical Memorandum 105281

Heats of Formation of BCC Binary Alloys

Guillermo Bozzolo
Analex Corporation
Brook Park, Ohio

John Ferrante
Lewis Research Center
Cleveland, Ohio

and

John R. Smith
General Motors Research Laboratories
Warren, Michigan

December 1991

NASA

HEATS OF FORMATION OF BCC BINARY ALLOYS

Guillermo Bozzolo
Analex Corporation
3001 Aerospace Parkway
Brook Park, Ohio 44142-1003

John Ferrante
National Aeronautics and Space Administration
Lewis Research Center
Cleveland, Ohio 44135-3191

John R. Smith
Physics Department
General Motors Research Laboratories
Warren, Michigan 48090-9055

Abstract

We apply the method of Bozzolo, Ferrante and Smith for the calculation of alloy energies for bcc elements. The heat of formation of several alloys is computed with the help of the Connolly-Williams method within the tetrahedron approximation. The dependence of the results on the choice of different sets of ordered structures is discussed.

Introduction

Recently, a new semiempirical method for calculating defect energetics in metallic alloys was introduced by Bozzolo, Ferrante and Smith (BFS)[1]. This technique, which builds on the ideas of Equivalent Crystal Theory (ECT)[2] was successfully applied to the study of heat of formation and lattice parameters of fcc alloys as a function of alloy composition. BFS is a quantitatively accurate and computationally simple technique for determining the energetics of ordered multicomponent structures. Although there has been extensive calculations for fcc alloys, similar results for bcc alloys have been limited. This is in part due to possible limitations in application of such approaches to bcc metals. Since alloys of bcc metals are important in structural materials, the present work represents an important contribution to the calculation of defect energies in alloys. In this effort, we apply BFS to the study of bcc-based binary alloys using the method of Connolly and Williams (CWM)[3] for the study of the energetics of disordered structures within the tetrahedron approximation.

In Section 2 we present the BFS method and discuss the application of CWM to several choices of ordered structures. An application to selected bcc-based binary alloys is discussed in Section 3. Conclusions are drawn in Section 4.

Formalism

In BFS, the energetics of binary alloys is described in terms of pure metal properties and only two experimentally (or theoretically) determined alloys properties. We build on the formulation of ECT by dividing the total energy of the alloy into a chemical energy and a strain or structural energy. The strain energy associated with a given atom is computed as if all of its neighbors were of the same atomic species. It arises from neighbor locations being different from in the elemental single-crystal environment. The remainder of the total energy is defined to be the chemical energy, which is due to some of an atom's neighbors being of a different atomic species. We now proceed to outline the procedure for calculation of heats of formation versus concentration for alloys with multiple atomic species. With this procedure, the binding energy curve as a function of volume is obtained from which the bulk properties of specified alloys can be extracted. The application of this technique to different crystallographic structures is straightforward. In this work, we concentrate on bcc-based binary alloys.

Consider a cell containing N_X atoms of atomic species X, $(X = A, B, ...)$, so that the total number of atoms in this cell is given by $N = \sum_X N_X$. The heat of formation of this cell is

$$\Delta E_{cell} = E_{cell} - \sum_X N_X E_X \tag{1}$$

where E_{cell} is the total energy of the cell and E_X is the cohesive energy of an atom of species X in a pure crystal of its own species. If $E'(i, X)$ denotes the energy of the i-th atom in the cell $(i = 1, ..., N_X)$ of species X then

$$\Delta E_{cell} = \sum_X \sum_{i=1}^{N_X} e_{i,X}. \tag{2}$$

where the energy difference $e_{i,X} = E'(i,X) - E_X$, has a strain and a chemical energy contribution, linked by a coupling factor $g_{i,X}$ that ensures that the chemical energy contribution vanishes for large interatomic distances:

$$e_{i,X} = e^S_{i,X} + g_{i,X} e^C_{i,X} \tag{3}$$

In order to compute the strain energy, $e^S_{i,X}$, we just 'flip' every atom surrounding atom (i,X) into an atom of the same species X, and perform a regular ECT calculation[2]. The equivalent lattice parameter $a^S_{i,X}$ is determined by solving the appropriate ECT equation applied to atom (i,X) in the defect (but pure) crystal. Then,

$$e^S_{i,X} = E^X_C \left[1 - (1 + a^{S*}_{i,X}) e^{-a^{S*}_{i,X}}\right], \quad a^{S*}_{i,X} = (a^S_{i,X} - a^X_e)/l_X. \tag{4}$$

where a^X_e denotes the lattice constant of a pure X crystal and E^X_C the corresponding cohesive energy.

In Eq. (3), the strain and chemical energies are coupled nonlinearly. The coupling function $g_{i,X}$ guarantees that the chemical contribution will vanish with increase in interatomic spacings, as it should. We define the coupling function in terms of the scaled equivalent lattice parameter of the strained crystal as follows

$$g_{i,X} = e^{-a^{S*}_{i,X}} \tag{5}$$

For the chemical energy contribution $e^C_{i,X}$, we keep the actual chemical composition of the cell (i.e., A, B, C in proper proportions for the alloy) , but we force the atoms surrounding atom (i,X) to be located in the lattice sites of a pure crystal of species X. Thus, we are including the effect of changing a neighbor to an A, B or C atom). Two similar

ECT calculations are then performed:

$$e^C_{i,X} = e^C_{i,X}(\{\Delta_{Y,X}\}) - e^C_{i,X}(0). \tag{6}$$

For the first term, $e^C_{i,X}(\{\Delta_{Y,X})\}$, the chemical perturbation is included in the appropriate values of the set of parameters $\{\Delta_{Y,X}\}$ which include the effects of changing the atomic species of a neighbor, where Y denotes the atomic species of a given neighbor of atom (i,X). In order to determine the parameters $\Delta_{Y,X}$ and $\Delta_{X,Y}$ for a given pair of atomic species (X,Y), two experimental values of *any* property of the X_xY_{1-x} alloy are needed. We choose to use the experimental heats of solution in the dilute limit which in most cases are readily available.

The equivalent lattice parameter $a^C_{i,X}$ is obtained by solving the corresponding ECT equation[2]

$$\begin{aligned} 12R_1^{p_X}e^{-\alpha_X R_1} + 6R_2^{p_X}e^{-(\alpha_X+\frac{1}{\lambda_X})R_2} &= \sum_Y N_{XY} r_1^{p_X} e^{-(\alpha_X+\Delta_{YX})r_1} \\ &+ \sum_Y M_{XY} r_2^{p_X} e^{-(\alpha_X+\frac{1}{\lambda_X}+\Delta_{YX})r_2} \end{aligned} \tag{7}$$

where R_1 and R_2 are the nearest-neighbor and next-nearest-neighbor distances in the equivalent crystal of lattice parameter $a^C_{i,X}$. The first term in the chemical energy, $e^C_{i,X}(\Delta_{Y,X})$ is then given by

$$e^C_{i,X}(\Delta_{Y,X}) = \gamma_{i,X} E_C^X \left[1 - (1 + a^{C*}_{i,X})e^{-a^{C*}_{i,X}}\right], \quad a^{C*}_{i,X} = (a^C_{i,X} - a^X_e)/l_X \tag{8}$$

with $\gamma_{i,X} = 1$ if $a^{C*}_{i,X} > 0$ and $\gamma_{i,X} = -1$ otherwise. The second term in Eq(8) is obtained by a similar procedure, but setting all the perturbative parameters $\{\Delta_{Y,X}\}$ equal to zero. This is done in order to free the chemical energy from any structural defect information,

retaining only the contribution of the chemical composition of the surroundings of atom (i, X).

In this work, we are concerned with calculating the heats of formation of the bcc-based ordered binary alloys $A_x B_{1-x}$. If no relaxation of the individual atomic sites is allowed, then the strain energy is simply

$$e_X^S = E_C^X \left[1 - (1 + a_X^{S*})\right] e^{-a_X^{S*}}, \quad a_X^{S*} = (r - a_e^X)/l_X. \tag{9}$$

where r is the actual interatomic distance of the alloy. Within this approximation, the second term in the chemical energy (Eq.(6)) vanishes, leaving us only with the computation of the first term, $e_X^C(\Delta)$. For a given ordered structure m, the ECT equation for the equivalent lattice parameter a_X^C (Eq.(8)) is

$$\begin{aligned} 12R_1^{p_X} e^{-\alpha_X R_1} + 6R_2^{p_X} e^{-(\alpha_X + \frac{1}{\lambda_X})R_2} &= N_{XX} r_1^{p_X} e^{-\alpha_X r_1} + N_{XY} r_1^{p_X} e^{-(\alpha_X + \Delta_{YX})r_1} \\ &+ M_{XX} r_2^{p_X} e^{-(\alpha_X + \frac{1}{\lambda_X})r_2} \\ &+ M_{XY} r_2^{p_X} e^{-(\alpha_X + \frac{1}{\lambda_X} + \Delta_{YX})r_2} \end{aligned} \tag{10}$$

with $R_1 = \frac{\sqrt{3}}{2} R_2; R_2 = a_X^C; r_1 = \frac{\sqrt{3}}{2} r_2; r_2 = a_e^X$. The parameters p_X, α_X and λ_X are listed in Ref. 2 and the coefficients N_{XX}, N_{XY}, M_{XX} and M_{XY} depend on the different ordered structures considered.

As in previous applications, we will use the heats of solution in the dilute limit as the experimental input for determining the parameters Δ_{AB} and Δ_{BA}. In order to compute the heats of formation of the disordered alloys, we use the Connolly-Williams method[3]. This method is based on a formal expression for the total energy first derived by Sanchez[4], where the total energy of a particular configuration m of a binary alloy consisting of atoms A and

B on a lattice of fixed symmetry is given by

$$\Delta E_m(r) = \sum_{\gamma} v_\gamma(r) \xi_\gamma^m \tag{11}$$

where $v_\gamma(r)$ are many-body potentials, the ξ_γ^m are multisite correlation functions defined on a γ-type cluster, r is the lattice parameter and the sum includes all γ-type clusters on the lattice. The multisite correlation functions are defined as

$$\xi_\gamma = \frac{1}{N_\gamma} \sum_{\{n_i\}} \sigma_{n_1} ... \sigma_{n_\gamma} \tag{12}$$

where σ_n is a spinlike variable which takes the values $+1$ and -1 depending on whether the lattice point n is occupied by an A or B atom , and N_γ is the total number of γ-type clusters.

The many-body potentials $v_\gamma(r)$ are obtained by inversion of Eq. (11), which implies the existence of a maximum cluster γ_{max} beyond which the $v_\gamma(r)$ are supposed to be negligible. Thus, for a certain set of ordered structures α and by arbitrarily truncating the summation in Eq. (12), the many-body potentials are

$$\begin{aligned} v_\gamma(r) &= \sum_m \left(\xi_\gamma^m\right)^{-1} \Delta E_m(r) \ , \ \phi \le \gamma \le \gamma_{max} \\ v_\gamma(r) &= 0 \quad , \quad \gamma_{max} < \gamma < \infty \end{aligned} \tag{13}$$

where ϕ represents the empty cluster. Recently[5], the CWM was extended to include more ordered structures and cluster sizes than the ones originally proposed[3] . Multisite correlations for the most common bcc and fcc based superstructures were also given[5]. Table 1 lists the correlations included in the tetrahedron truncation of the CWM for some structures on the bcc lattice. Table 2 shows the coefficients N_{XX}, N_{XY}, M_{XX} and M_{XY} needed to solve Eq. (10) for all the possible ordered structures included in Table 1. These ordered

structures are derived from the tetrahedron cluster shown in Fig. 1: α and γ are on body centers and β and δ are on cube edges. When $\alpha = \gamma$ and $\beta = \delta$ the structure is called $B2$. The B32 structure is derived when $\alpha = \delta \neq \beta = \gamma$ and the DO_3 structure is obtained when $\beta = \delta \neq \alpha \neq \gamma$.

In this work, we considered different choices of ordered structures, as well as the type of clusters included in Eq. (12). Being that the experimental input is, obviously, the same for all cases studied, a comparison with available experimental data for the heats of formation of binary alloys[6] should give us an indication of the preferred ordered structures for a given binary alloy.

The different choices are related to the two possible ordered structures at 50 % composition (B2 and B32) and the corresponding pair multisite correlation functions (ξ_2 and ξ_3). We will denote the cases studied as follows: (*i*) B32/ξ_2: includes the B32 ordered structure and the ξ_2 correlation function (nearest-neighbor pair), leaving out the $B2$ structure as well as the ξ_3 function (next-nearest-neighbor pair); (*ii*) B32/ξ_3: includes the ordered structure B32 and the ξ_3 function, leaving out B2 and ξ_2; (*iii*) B2/ξ_2: includes B2 and ξ_2, leaving out B32 and ξ_3 and (*iv*) B2+B32/$\xi_2 + \xi_3$: includes all the structures and functions listed in Table 1. In each case, the excess energy $\Delta E_m(r)$ for the corresponding ordered structures is obtained with Eq. (2). Within the tetrahedron approximation, this calculation involves just a few atoms, as indicated in Table 2.

Following CWM, the excess energy for the disordered alloys A_xB_{1-x} is given by

$$\Delta E_D(r,x) = \sum_{\gamma}(1-2x)^{n_\gamma} v_\gamma(r) \tag{14}$$

where n_γ is the number of sites contained in the γ cluster. For each choice of ordered

structures and multisite correlation fuctions we have different many-body potentials

$$v_\gamma(r) = \sum_m \left(\xi_\gamma^m\right)^{-1} \Delta E_m(r). \tag{15}$$

Replacing Eq. (15) in Eq. (14), we can write $\Delta E_D(r,x)$ for each one of the cases studied as

$$\Delta E_D(r,x) = \sum_m c_m(x) \Delta E_m(r) \tag{16}$$

where the sum runs over the appropriate ordered structures included in each case considered and the polynomials $c_m(x)$ are also dependent on the clusters and structures included in each case. Table 3 lists the polynomials $c_m(x)$ for the reduced basis sets (*i*), (*ii*) and (*iii*) and Table 4 displays the corresponding polynomials for the general case (all structures and multisite correlation functions included in Table 1). Finally, the heat of formation for a given concentration x is obtained by finding the minimum value of $\Delta E_D(r,x)$.

Results and Discussion

In this section we present results for selected bcc-based alloys which display quite different behavior. For the four systems studied, we used the experimental values of the heats of solution in the dilute limit[6], listed in Table 5. Table 6 displays the values of p, α, l and E_C for the pure elements[2], needed to solve Eqs. (4)-(10). Table 7 shows the values of Δ_{AB} and Δ_{BA} one obtains with our procedure for the different choices of basis sets described in the previous section.

The parameters Δ_{AB} and Δ_{BA} can be taken as 'perturbations' to the pure-element α's listed in Table 6, trying to simulate the interaction between two atoms of different species. In all cases, these quantities are small compared to the pure-element α's, and, surprisingly, rather insensitive to the different choices of basis sets. However, these small differences translate into a noticeable change in the heat of formation versus concentration curves obtained for each choice of basis set, as can be seen in Fig. 2.

Fig. 2.a shows the results obtained for Cr-Fe alloys where the regular, symmetric behavior of the heat of formation curve is accurately reproduced by using the basis set (*iii*), where a B2 structure is included. Although there is no known ordered phase of Cr-Fe with the B2 structure, the fact that the choice (*iii*) is favored over the others can be taken as an indication of the possible existence of such phases. This assumption is further validated by similar results for Fe-V alloys (Fig. 2.b) where, again, basis set (*iii*) best approximates the available experimental values of the heat of formation[6]. In this case, there is some experimental evidence that such an ordered phase exists[6,7].

The predictions for Cr-Mo alloys show a drastic change in behavior as compared to Cr-Fe, although both systems display similar features in the experimental values of the heat

of formation. Fig. 2.c shows the theoretical results. In this case, the basis sets (*i*) and (*ii*) yield comparable results, predicting a preference for a B32 structure, although there are no known ordered phases of these alloys.

Of the four examples shown in this work, Cr-V (Fig. 2.d) displays the most surprising features, therefore providing a severe test to the sensitivity and accuracy of our method. In the large body of experimental data for binary alloys, Cr-V is one of the very few to display the irregularities seen in the heat of formation vs. concentration curve, characterized by a sudden change in curvature for a small range of concentrations. As it was the case for Cr-Mo, this feature of Cr-V is approximately reproduced *only* by the results generated with the choice of the basis set (*ii*). Once again, no ordered phase is known, but the clear distinction between the different basis set choices shown in Fig. 2.d can be taken as an indication of the crystallographic structure of these alloys.

The fact that we used the experimental heats of solution in the dilute limit (i.e., the derivative of the heat of formation at $x = 0$ and $x = 1$) might lead one to believe that that choice somehow predetermines the behavior of the heat of formation curves. The examples shown in this work obviously contradict this fact: all four curves (for each choice of basis set) were obtained with the *same* values of the heats of solution. However, their behavior for the whole range of concentration is quite different in each case.

The explanation for the particular features of the heat of formation vs. concentration curves is not then in the heats of solution, which is our only experimental input, but in the delicate balance between the strain and chemical energies, as defined in our formalism. Except for the case of Cr-Fe, where the small lattice mismatch results in an almost negligible strain energy, in all the other cases the heat of formation predicted with our method is

obtained from large competing strain and chemical energy contributions.

Fig. 3 displays these contributions for the four systems considered in Fig. 2, showing the results obtained with the best basis set choice for each system, as discussed before. The apparent similarity seen in Cr-Fe and Cr-Mo for their heats of formation, arises from quite different strain and chemical energy contributions: while the positive chemical energy is mainly responsible for the heat of formation for Cr-Fe alloys (Fig. 3.a), a large negative chemical energy in Cr-Mo (Fig. 3.c) is necessary to balance a large strain energy contribution, absent in Cr-Fe. Also, the symmetry seen in the heat of formation curve for Cr-Mo is a result of completely different regimes in the strain and chemical energies: linear for Mo-rich systems and with a pronounced curvature for Cr-rich alloys. Fig. 3.b shows, for Fe-V, how the chemical energy is solely responsible for the axis-crossing seen in the heat of formation curve.

As noted before, Cr-V provides the appropriate grounds for testing the sensitivity of this method. Fig. 3.d displays the strain and chemical energy contributions for the Cr-V systems. One can see how a barely noticeable flattening in the chemical energy contribution is the source of the unusual feature seen in the heat of formation curve. These results correspond to the basis set (*ii*), which best approximates the experimental results. Finally, Fig. 4 expands on the results shown in Fig. 3.d in that the strain and chemical energy contributions are displayed for all four basis sets. The strain energy contribution (independent of Δ_{CrV} and Δ_{VCr}) shows small differences due to the choice of different ordered structures. The chemical energy term dictates the behavior of the heat of formation as a function of concentration: the asymmetry seen in Fig. 3.d arises from the chemical behavior of the B32 structure.

Conclusions

In this work, we applied the semiempirical method of Bozzolo, Ferrante and Smith to the study of bcc-based alloys. The method was used to compute the total energy of ordered structures. The energetics of disordered alloys was studied with the CWM and several choices of basis sets were considered. Good agreement with experimental results for certain choices of basis sets gives an indication of the possible symmetries underlying the ordered compounds. The partition of the heat of formation into strain and chemical contributions provides some insight in the physical behavior of the systems studied.

Acknowledgements

Fruitful discussions with Prof. Herbert Schlosser are gratefully acknowleged. This work was partially supported by the Engineering Directorate, NASA Lewis Research Center.

References

[1]Guillermo Bozzolo and John Ferrante, N.A.S.A. Technical Publication (1991) (in press); Guillermo Bozzolo, John Ferrante and John R. Smith (to be published)

[2]John R. Smith and Amitava Banerjea, Phys. Rev. **B37** 10411 (1988); John R. Smith, Tom Perry, Amitava Banerjea, John Ferrante and Guillermo Bozzolo, Phys. Rev. B (in press)

[3]J. W. D. Connolly and A. R. Williams, Phys. Rev. **B27** 5169 (1983)

[4]T. Mohri, J. M. Sanchez and D. de Fontaine, Acta Metall. **33** 1171 (1985)

[5]M. Sluiter and P. E. A. Turchi, Phys. Rev. **B40** 11215 (1989)

[6]R. Hultgren, R. L. Orr, P. D. Anderson and K. K. Kelley in *Selected Values of the Thermodynamic Properties of Binary Alloys* (Wiley, N.Y., 1963).

[7]W. B. Pearson in *Handbook of Lattice Spacings and Structures of Metals* (Pergamon Press, 1967).

[8]S. -H. Wei, A. A. Mbaye, L. G. Ferreira and Alex Zunger, Phys. Rev. **B36** 4163 (1987)

[9]S. Takizawa, K. Terakura and T. Mohri, Phys. Rev. **B39** 5792 (1989)

TABLE 1. - CORRELATIONS INCLUDED IN THE TETRAHEDRON TRUNCATION OF THE CWM FOR SOME STRUCTURES ON THE BCC LATTICE

[The ξ_i with increasing index i, correspond to the empty cluster, the point, the nearest-neighbor (NN) pair, the next-nearest-neighbor (NNN) pair, the triangle formed by two NN pairs and one NNN pair, and the tetrahedron formed by four NN pairs and two NNN pairs.]

Structure	Composition	ξ_0	ξ_1	ξ_2	ξ_3	ξ_4	ξ_5
bcc	A	1	1	1	1	1	1
DO_3	A_3B	1	$\frac{1}{2}$	0	0	$-\frac{1}{2}$	-1
B2	AB	1	0	-1	1	0	1
B32	AB	1	0	0	-1	0	1
DO_3	AB_3	1	$-\frac{1}{2}$	0	0	$\frac{1}{2}$	-1
bcc	B	1	-1	1	1	-1	1

TABLE 2. - COEFFICIENTS N_{XX}, N_{XY}, M_{XX}, and M_{XY}

Struc./Comp.	Atom	N_{AA}	N_{AB}	N_{BB}	N_{BA}	M_{AA}	M_{AB}	M_{BB}	M_{BA}
bcc/B	B(4)	0	0	8	0	0	0	6	0
DO_3/AB_3	A(1)	0	8	0	0	0	6	0	0
	B(2)	0	0	4	4	0	0	6	0
	B(1)	0	0	8	0	0	0	0	6
B2/AB	A(2)	0	8	0	0	6	0	0	0
	B(2)	0	0	0	8	0	0	6	0
B32/AB	A(2)	4	4	0	0	0	6	0	0
	B(2)	0	0	4	4	0	0	0	6
DO_3/A_3B	A(2)	4	4	0	0	6	0	0	0
	A(1)	8	0	0	0	0	6	0	0
	B(1)	0	0	0	8	0	0	0	6
bcc/A	A(4)	8	0	0	0	6	0	0	0

TABLE 3. - POLYNOMIALS $c_m(x)$ FOE CASES (i), (ii), AND (iii)

Struct.	Comp.	m	(i)	(ii)	(iii)
bcc	B	0	$1-4x+5x^2-2x^3$	$1-4x+7x^2-6x^3+2x^4$	$1-4x+7x^2-6x^3+2x^4$
DO_3	AB_3	1	$4x-12x^2+12x^3-4x^4$	$4x-12x^2+12x^3-4x^4$	$4x-12x^2+12x^3-4x^4$
B2	AB	2	-	-	$4x^2-8x^3+4x^4$
B32	AB	2	$8x^2-16x^3+8x^4$	$4x^2-8x^3+4x^4$	-
DO_3	A_3B	3	$4x^3-4x^4$	$4x^3-4x^4$	$4x^3-4x^4$
bcc	A	4	$-x^2+2x^3$	$x^2-2x^3+2x^4$	$x^2-2x^3+2x^4$

TABLE 4. - POLYNOMIALS $c_{in}(x)$ FOR CASE (iv)

Structure	Composition	m	(iv)
bcc	B	0	$1-4x+6x^2-4x^3+x^4$
DO_3	AB_3	1	$4x-12x^2+12x^3-4x^4$
B2	AB	2	$4x^2-8x^3+4x^4$
B32	AB	2	$2x^2-4x^3+2x^4$
DO_3	A_3B	3	$4x^3-4x^4$
bcc	A	4	x^4

TABLE 5. - EXPERIMENTAL HEATS OF SOLUTION E_{AB} AND E_{BA}

A	B	E_{AB}	E_{BA}
Cr	Fe	0.218	0.218
Fe	V	-0.102	0.807
Cr	V	-0.088	-0.189
Cr	Mo	0.215	0.323

TABLE 6. - INPUT PARAMETERS FOR BCC ELEMENTS

Element	p	l	α	λ	Cohesive Energy	Lattice Constant
Cr	6	0.254	2.889	0.714	4.10	2.88
Fe	6	0.277	3.124	0.770	4.29	2.86
V	6	0.305	2.726	0.857	5.31	3.03
Mo	8	0.262	3.420	0.736	6.82	3.15

TABLE 7. - PARAMETERS Δ_{AB} AND Δ_{BA}

A	B	Basis set	Δ_{AB}	Δ_{BA}
Cr	Fe	(i)	0.0445	0.0277
		(ii)	0.0443	0.0279
		(iii)	0.0447	0.0275
		(iv)	0.0448	0.0274
Fe	V	(i)	0.0751	-0.0644
		(ii)	0.0757	-0.0647
		(iii)	0.0768	-0.06515
		(iv)	0.0775	-0.0649
Cr	V	(i)	-0.0228	-0.0215
		(ii)	-0.0230	-0.02115
		(iii)	-0.0222	-0.0226
		(iv)	-0.0217	-0.0221
Cr	Mo	(i)	-0.0246	-0.0060
		(ii)	-0.0248	0.0060
		(iii)	-0.0238	-0.0143
		(iv)	-0.0230	-0.0075

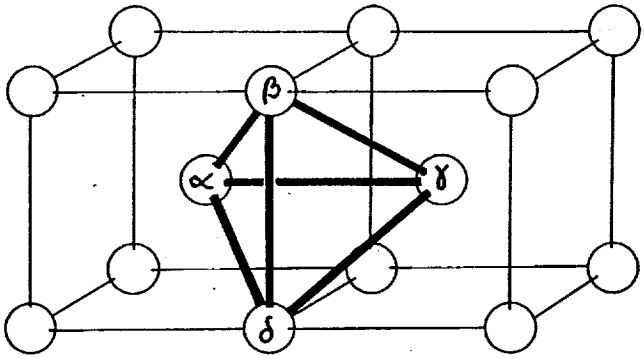

Figure 1.—Tetrahedron cluster in a bcc lattice (see text).

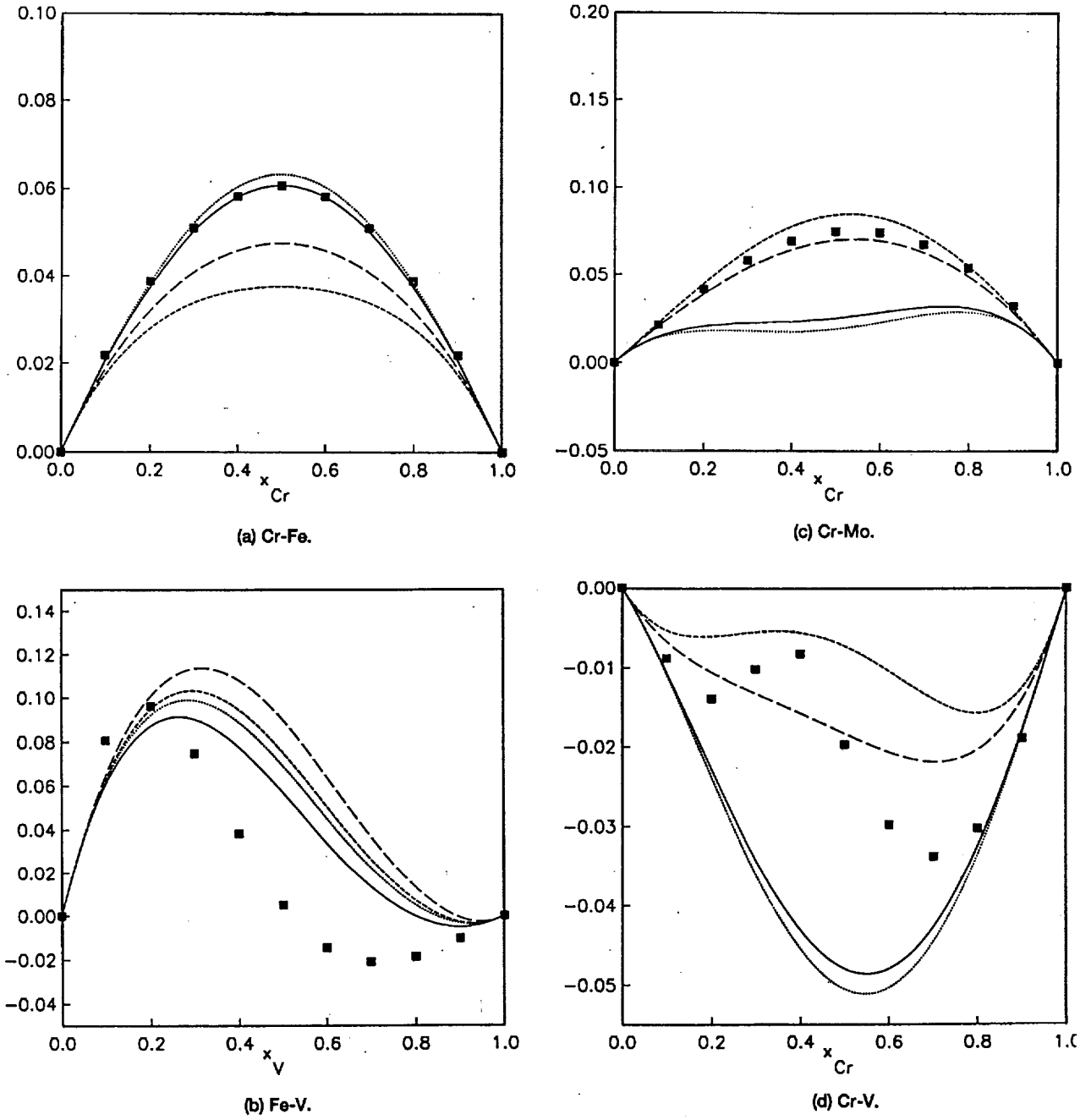

Figure 2.—Heat of formation versus concentration for different bcc-based alloys. In all cases, the solid squares indicate experimental values, and the different curves the results obtained using the basis sets and correlation functions described in the text: (i) B32/ξ_2 (long-dashed line), (ii) B32/ξ_3 (short-dashed line), (iii) B2/ξ_2 (solid line) and (iv) B32+B2/ξ_3 (dotted line).

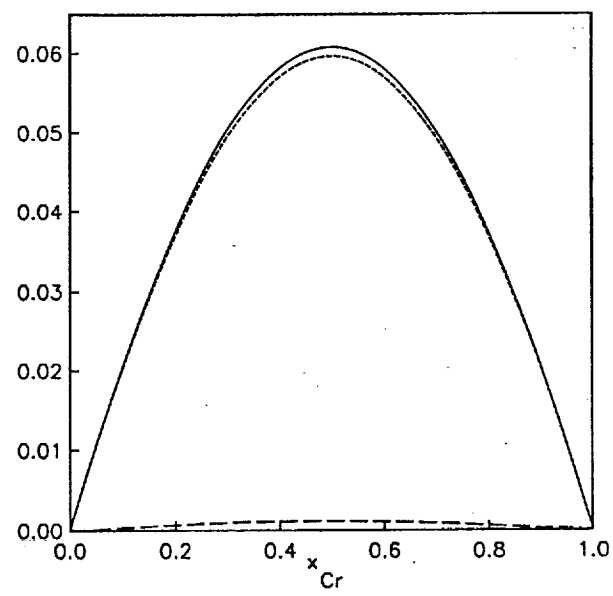

(a) Cr-Fe.

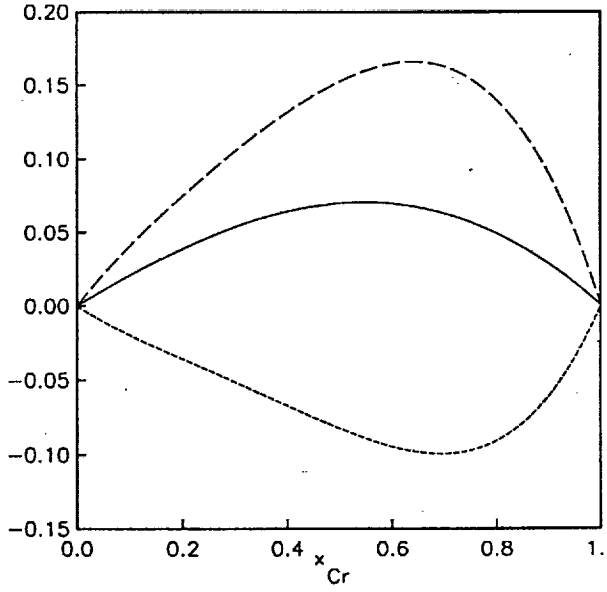

(c) Cr-Mo.

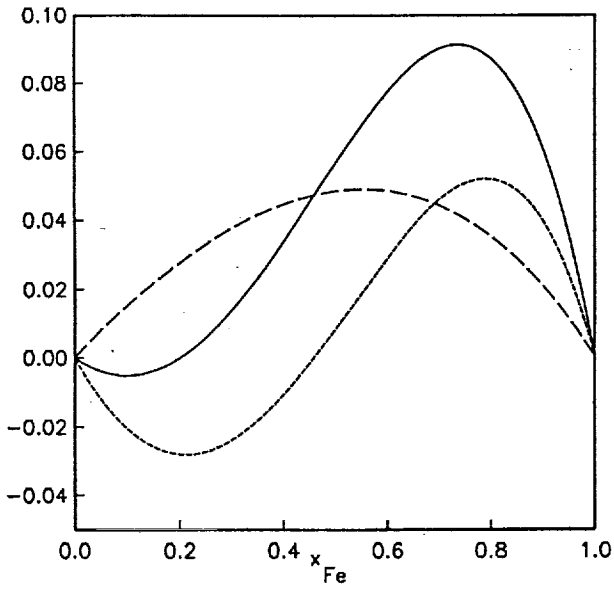

(b) Fe-V.

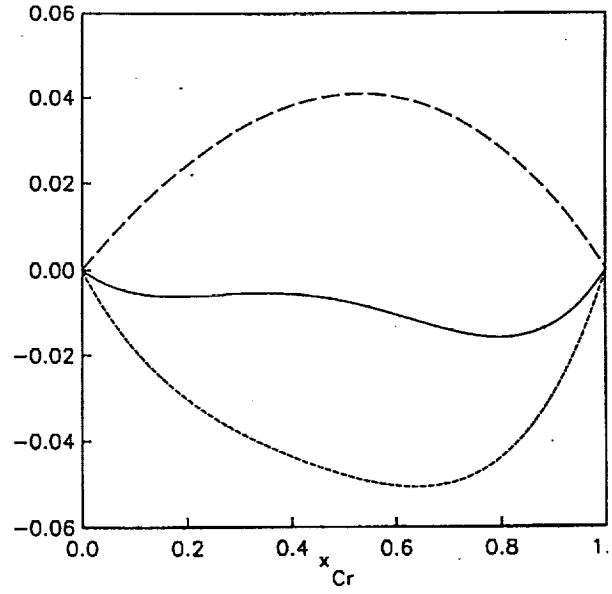

(d) Cr-V.

Figure 3.—Strain energy (long-dashed line) and chemical energy (short-dashed line) contributions to the heat of formation (solid curve).

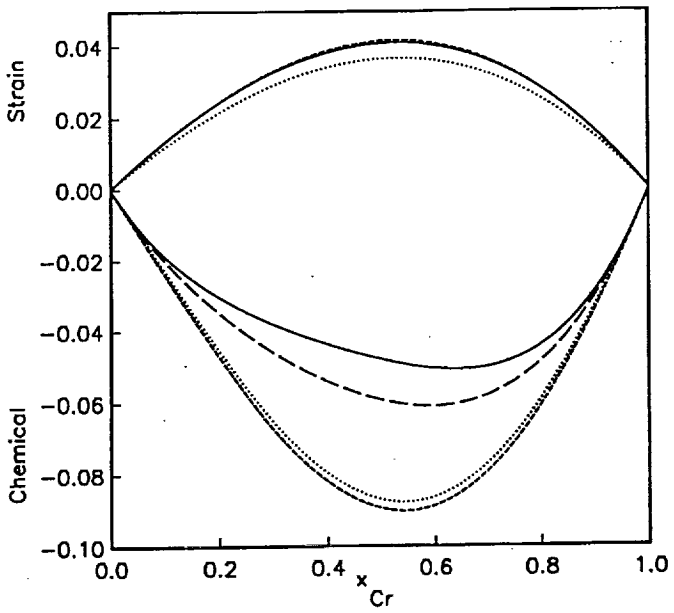

Figure 4.—Strain and chemical contributions to the heat of formation of Cr-V for different choices of ordered structures (see text): (i) (longdashed curves), (ii) solid curves, (iii) (short-dashed curves and(iv) (dottedcurves). The sum of these pairs of curves are shown in Fig. 2.d.

REPORT DOCUMENTATION PAGE

Form Approved
OMB No. 0704-0188

1. AGENCY USE ONLY (*Leave blank*)	2. REPORT DATE	3. REPORT TYPE AND DATES COVERED
	December 1991	Technical Memorandum

4. TITLE AND SUBTITLE

Heats of Formation of BCC Binary Alloys

5. FUNDING NUMBERS

WU-505-90-52

6. AUTHOR(S)

Guillermo Bozzolo, John Ferrante, and John R. Smith

7. PERFORMING ORGANIZATION NAME(S) AND ADDRESS(ES)

National Aeronautics and Space Administration
Lewis Research Center
Cleveland, Ohio 44135-3191

8. PERFORMING ORGANIZATION REPORT NUMBER

E-6588

9. SPONSORING/MONITORING AGENCY NAMES(S) AND ADDRESS(ES)

National Aeronautics and Space Administration
Washington, D.C. 20546-0001

10. SPONSORING/MONITORING AGENCY REPORT NUMBER

NASA TM-105281

11. SUPPLEMENTARY NOTES

Guillermo Bozzolo, Analex Corporation, 3001 Aerospace Parkway, Brook Park, Ohio 44142; John Ferrante, NASA Lewis Research Center; John R. Smith, General Motors Research Laboratories, Physics Department, Warren, Michigan 48090. Responsible person, John Ferrante, (216) 433-6069.

12a. DISTRIBUTION/AVAILABILITY STATEMENT

Unclassified - Unlimited
Subject Category 26

12b. DISTRIBUTION CODE

13. ABSTRACT (*Maximum 200 words*)

We apply the method of Bozzolo, Ferrante and Smith for the calculation of alloy energies for bcc elements. The heat of formation of several alloys is computed with the help of the Connolly-Williams method within the tetrahedron approximation. The dependence of the results on the choice of different sets of ordered structures is discussed.

14. SUBJECT TERMS

Alloys; Heat of formation

15. NUMBER OF PAGES

22

16. PRICE CODE

A03

17. SECURITY CLASSIFICATION OF REPORT	18. SECURITY CLASSIFICATION OF THIS PAGE	19. SECURITY CLASSIFICATION OF ABSTRACT	20. LIMITATION OF ABSTRACT
Unclassified	Unclassified	Unclassified	